

## Growth and Characterization of Sodium Penta Fluoro Antimonate –Inorganic NLO Crystal

<sup>1</sup>\*C. Besky Job, <sup>1</sup>J. Anbuselvam, <sup>1</sup>R. Shabu, <sup>2</sup>S. Paul Raj

<sup>1</sup>Department of Physics and Research Centre, Scott Christian College (Autonomous), Nagercoil-629 003, Tamil Nadu, India.

<sup>2</sup>Department of Physics and Research Centre, St. Xavier's College (Autonomous), Palayamkottai-627 002, Tamil Nadu, India.

**Abstract:** Sodium Penta Fluoro Antimonate crystal has attracted the researchers for its superionic conductivity and its electro optic properties. It has been grown by the conventional slow evaporation technique. The single crystal X-ray diffraction studies confirms the crystal belongs to Orthorhombic system with lattice parameters  $a = 5.453 \text{ \AA}$ ,  $b = 8.006 \text{ \AA}$ ,  $c = 11.133 \text{ \AA}$ ,  $\alpha = \beta = \gamma = 90^\circ$  and has the space group of  $P2_12_12_1$ . The FTIR spectrum analysis has confirmed the functional groups present in the grown crystal, especially the Sb-F bond. UV-Vis spectral studies performed the lower cut off wavelength of the grown  $\text{Na}_2\text{SbF}_5$  crystal as 311 nm in the UV region. The band gap energy of the grown crystal has been found to be 5.3 eV using Tauc's plot. Penn gap, Fermi gap and polarizability of the grown crystal have been estimated from the dielectric studies. It is noticed that the SHG efficiency of the grown crystal is 0.265 times that of the KDP crystal.

**Keywords:** Sodium Penta Fluoro Antimonate –Inorganic NLO Crystal.

### 1. Introduction

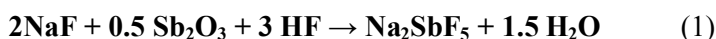
The study of physiochemical properties of inorganic fluorides is gaining interest because of the extensive possibilities for their applications in optical instruments and laser technology [1]. Monofluorides (AF) and Pentafluorides ( $\text{MF}_5$ ) form a variety of compounds with general formulas  $\text{AMF}_6$ ,  $\text{A}_2\text{MF}_7$ ,  $\text{A}_3\text{MF}_8$ ,  $\text{AM}_2\text{F}_{11}$ ,  $\text{AM}_3\text{F}_{16}$  and  $\text{AM}_4\text{F}_{21}$  [2]. Also it is known for long time that metal fluorides dissolve in anhydrous hydrogen fluoride (aHF) acidified with Lewis acids ( $\text{AsF}_5$ ,  $\text{SbF}_5$ ) [3]. Antimony pentafluoride,  $\text{SbF}_5$  is the strongest Lewis acid in anhydrous hydrogen fluoride (aHF) [4-5]. Trivalent Antimony Fluoride complexes represent an extensive class of inorganic compounds, among which many substances exhibits unusual electro physical, optical and other properties [6-8]. It has also been reported that a number of fluoride crystals showed super ionic conductivity [9-11]. Characterization studies on various fluoro antimonate family crystals like Tri Ammonium Fluoro Di Antimonate ( $(\text{NH}_4)_3\text{Sb}_2\text{F}_9$ ) [12],  $\text{NH}_4\text{Sb}_3\text{F}_{10}$  [13],  $\text{NH}_4\text{Sb}_2\text{F}_7$  [14], Lithium Hexa Fluoro Diantimonate ( $\text{LiSb}_2\text{F}_7$ ) and  $\text{LiSbF}_4$  [15],  $\text{Ni}(\text{SbF}_6)_6$  [16],  $\text{CsSbF}_5(\text{OH})$  and  $\text{CsSbF}_4(\text{OH})_2$  [17],  $\text{RbSb}_2\text{F}_7$  [18],  $\text{KSbF}_4$  [19-21] and  $\text{KSb}_4\text{F}_{13}$  [22-23]. Researchers have been devoted so many pages on the characterization studies of sodium fluoro antimonate crystals such as  $\text{NaSbF}_4$  [24],  $\text{NaSb}_2\text{F}_7$  [25],  $\text{NaSb}_3\text{F}_{10}$  [26],  $\text{Na}_3\text{Sb}_5\text{F}_{18}$  [27] and  $\text{Na}_2\text{SbBF}_8$  [28]. Many attempts have been made to study the growth and physical properties of different penta fluoro antimonate crystals such as Potassium Penta Fluoro Antimonate ( $\text{K}_2\text{SbF}_5$ ) [29-31], Ammonium Penta Fluoro Antimonate ( $(\text{NH}_4)_2\text{SbF}_5$ ) [32], Strontium Penta Fluoro Antimonate ( $\text{SrSbF}_5$ ) [33] and Barium Penta Fluoro antimonate ( $\text{BaSbF}_5$ ) [34]. The characterization studies on Sodium Penta Fluoro Antimonate

crystal( $\text{Na}_2\text{SbF}_5$ ) such as single crystal XRD [35-36], FTIR [37], micro hardness [38] and NLO studies [39-40] have been already reported by many researchers.

In the present investigation Sodium Penta Fluoro Antimonate crystal ( $\text{Na}_2\text{SbF}_5$ ) has been grown by the conventional slow evaporation method. The grown crystal has been subjected to various characterization techniques such as Powder XRD, Single crystal XRD, FTIR, UV, Dielectric, and NLO studies.

## 2. Crystal Growth

The stoichiometric mixture of high purity AR grade NaF,  $\text{Sb}_2\text{O}_3$  and HF were used as starting material in a molar ratio of 2:0.5:3. The calculated amounts of the reactants were thoroughly dissolved in deionized water and stirred well for about 6 hrs. This was filtered to remove suspended impurities and allowed to crystallize. The chemical equation governing the reaction is,



The homogenous solution was kept in PVC containers for slow evaporation. Single crystals with good transparency are obtained in a period of 2 weeks and are shown in fig. 1.

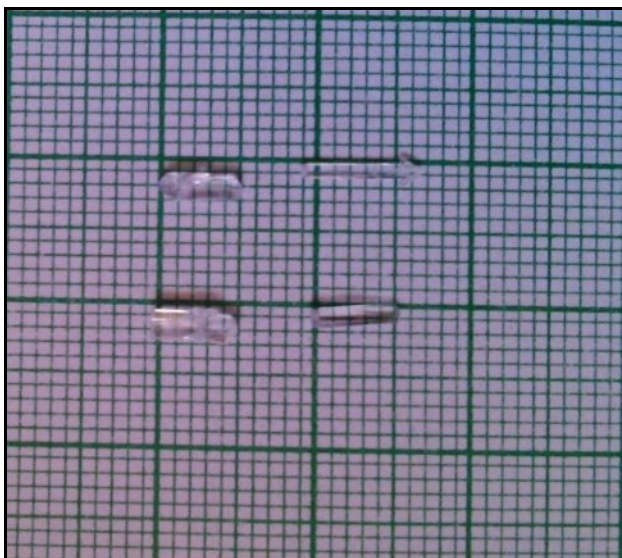


**Fig. 1** The photograph of the grown  $\text{Na}_2\text{SbF}_5$  crystal

## 3. Xrd Analysis

Powder X-ray diffraction analysis has been carried out using Bruker AXS D8 Advance Powder X-ray Diffractometer using  $\text{CuK}\alpha$  radiation ( $\lambda = 1.5406 \text{ \AA}$ ) scanned over the range of  $10$  to  $80^\circ$  at a scan rate of  $1^\circ/\text{min}$ . The standard and observed powder XRD pattern of the grown  $\text{Na}_2\text{SbF}_5$  crystal is shown in Fig. 2. The well defined peaks confirm the crystalline nature of the grown crystal. The observed powder XRD spectrum of the grown crystal has been compared with the JCPDS file (27-0733), noticed that it has very good agreement with the standard powder XRD spectrum. The peak corresponding to (102) plane has a maximum intensity of 1110.

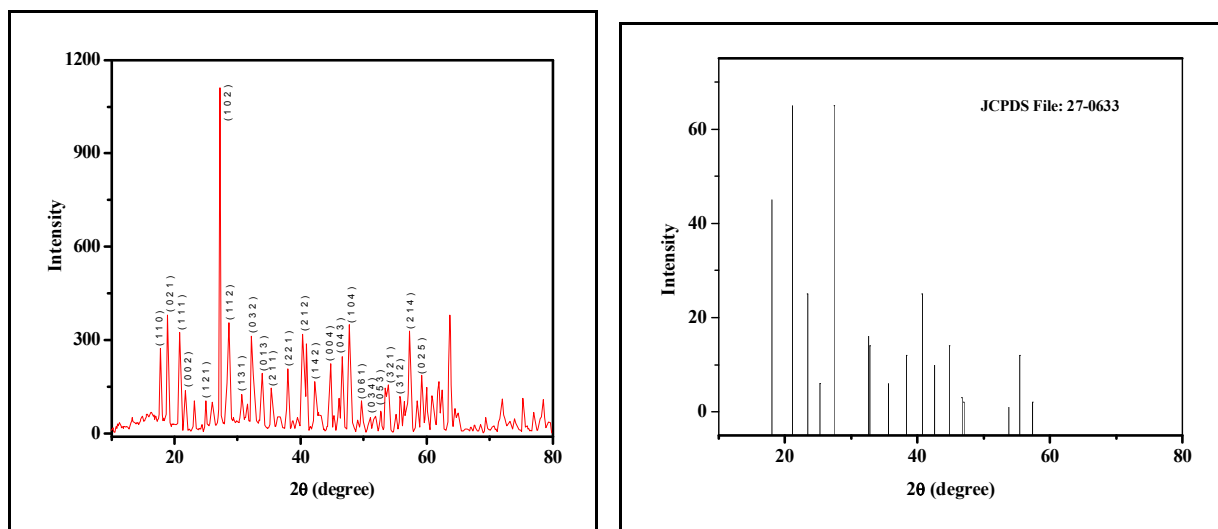


**Fig.2 The standard and observed indexed Powder XRD pattern of the grown Na<sub>2</sub>SbF<sub>5</sub> crystal**

Single crystal x-ray diffraction studies have been carried out using ENRAF NONIUS CAD4 single crystal x-ray diffractometer. The single crystal XRD data of Na<sub>2</sub>SbF<sub>5</sub> crystal indicates that it crystallizes in orthorhombic system with P<sub>2</sub>1<sub>2</sub>1 space group. The observed lattice constants are  $a = 5.453 \text{ \AA}$ ,  $b = 8.006 \text{ \AA}$ ,  $c = 11.133 \text{ \AA}$ ,  $\alpha = \beta = \gamma = 90^\circ$  and volume =  $486.1 \text{ \AA}^3$ , which agree well with the reported values [41].

#### 4. Ftir Analysis

The observed FTIR spectrum of Na<sub>2</sub>SbF<sub>5</sub> crystal has been recorded using Perkin Elmer Spectrometer using KBr pellet technique in the wavelength range from  $4000 \text{ cm}^{-1}$  to  $400 \text{ cm}^{-1}$ . The FTIR spectrum of the grown Na<sub>2</sub>SbF<sub>5</sub> crystal is shown in Fig. 3.

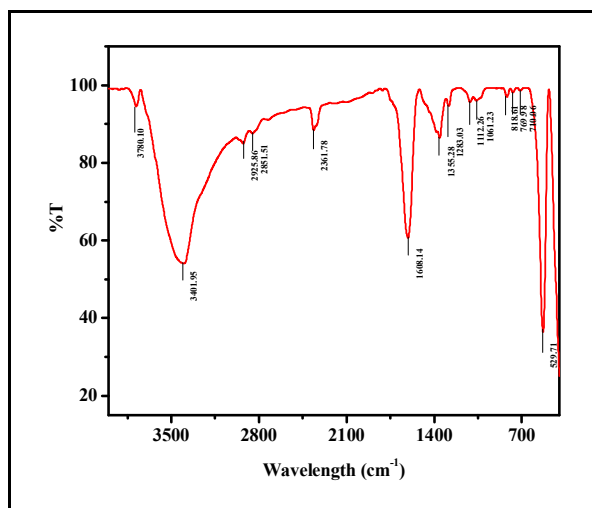


**Fig. 3 FTIR spectrum of the grown Na<sub>2</sub>SbF<sub>5</sub> crystal**

Infrared spectroscopy is effectively used to determine the functional groups present in the crystal [42]. The O-H stretching vibrations appear as intense broad envelope in the higher energy region with maxima at  $3780$  and  $3402 \text{ cm}^{-1}$ . The absorption bands at  $1608 \text{ cm}^{-1}$  is related to deformation of water molecules with inequivalent OH bonds [43]. The existence of Sb-O bond is clearly evident from the sharp peaks at  $1355$ ,  $1283$ ,  $1112$  and  $1061 \text{ cm}^{-1}$  [44]. We assume that the sharp peaks are seen at  $819$ ,  $770$  and  $711 \text{ cm}^{-1}$  reveals the presence of Na-Sb bond. The symmetric stretching vibration of Sb-F bond is positioned at  $530 \text{ cm}^{-1}$  [45-46].

5. Uv – Vis - Spectral Analysis

The UV–Vis–transmission spectrum of the crystal was recorded using Perkin Elmer Lambda 35 UV Vis spectrometer in the wavelength range of 190–1100 nm. The optical transmittance spectrum of the grown Na<sub>2</sub>SbF<sub>5</sub> crystal is shown in Fig. 4. The grown crystal exhibits transmittance in entire visible region with lower UV cut-off wavelength found to be around 310 nm. This property attests the suitability of the crystal for nonlinear optical applications [47].

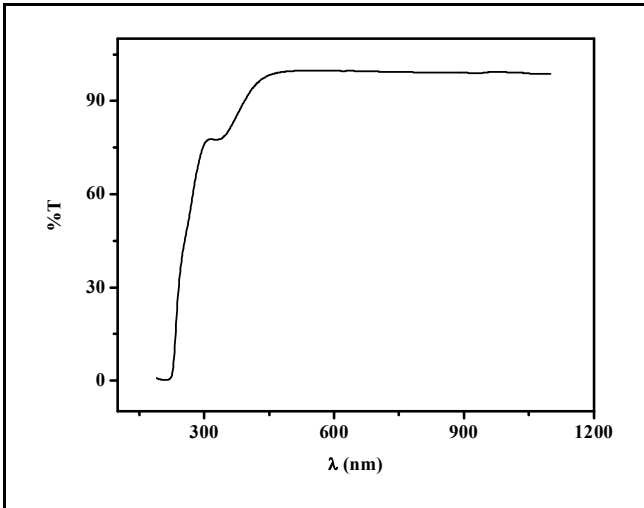


Fig.4 The optical transmittance spectrum of the grown Na<sub>2</sub>SbF<sub>5</sub> crystal

The optical absorption coefficient ( $\alpha$ ) was calculated using the following relation,

$$\alpha = \frac{2.303 \log\left(\frac{1}{T}\right)}{d}$$

Where T is the transmittance, d is the thickness of the crystal. The plot of optical absorption coefficient vs wavelength for the grown Na<sub>2</sub>SbF<sub>5</sub> crystal is presented in Fig. 5.

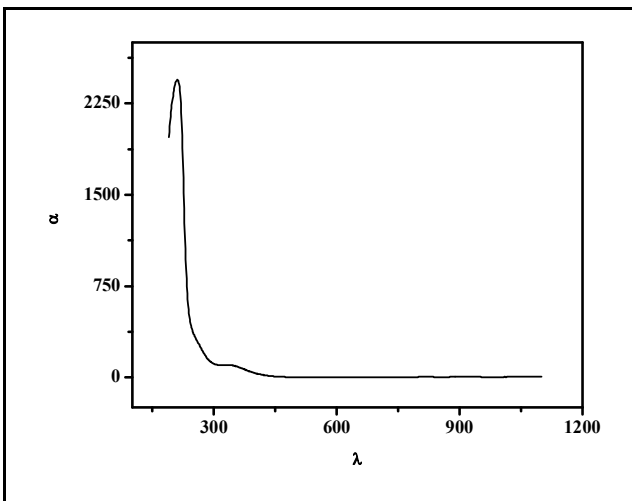


Fig.5 Plot between optical absorption coefficient vs wavelength of the grown Na<sub>2</sub>SbF<sub>5</sub> crystal

The crystal under study has an absorption coefficient ( $\alpha$ ) obeying the following relation for high photon energies ( $h\nu$ ),

$$\alpha h\nu = B^2(h\nu - E_g)^n \tag{3}$$

where  $\alpha$  is the absorption coefficient and  $\nu$  is the frequency,  $E_g$  is the optical band gap, B is a constant and n is an index which can be assumed to have values of 1/2, 3/2, 2 and 3, depending on the nature of electronic transition responsible for the absorption, i.e.,  $n = 1/2$  for the direct allowed transition (high energy part of the spectra),  $n = 3/2$  for forbidden direct transition,  $n = 2$  for the indirect allowed transition (low energy part of the spectra) and  $n = 3$  for forbidden indirect transition [48]. The variation of  $(\alpha h\nu)^n$  with  $h\nu$  (Tauc plot), for these crystals, is shown in Fig. 6. The value of  $E_g$  for the sample have been calculated by extrapolating the linear region of the curves to meet the  $h\nu$  axis at  $(\alpha h\nu)^n = 0$ , and are estimated as 5.3 eV.

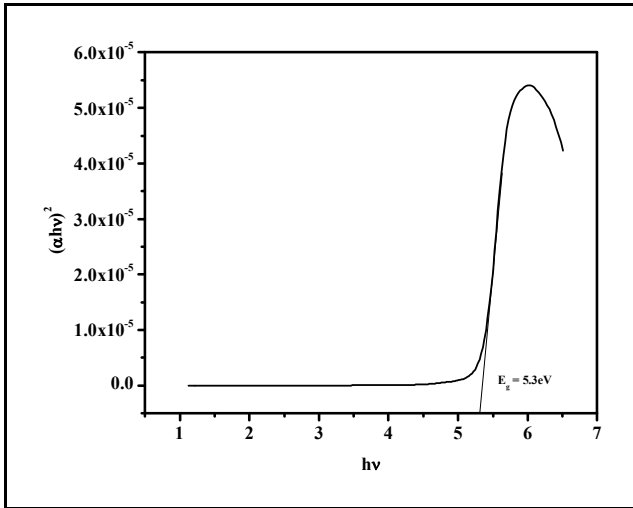


Fig.6 Tauc's plot of the grown  $\text{Na}_2\text{SbF}_5$  crystal

The plot of variation of extinction coefficient with wavelength was presented in Fig. 7. Extinction coefficient (K) can be obtained from the following equation,

$$K = \frac{\lambda\alpha}{4\pi} \quad (4)$$

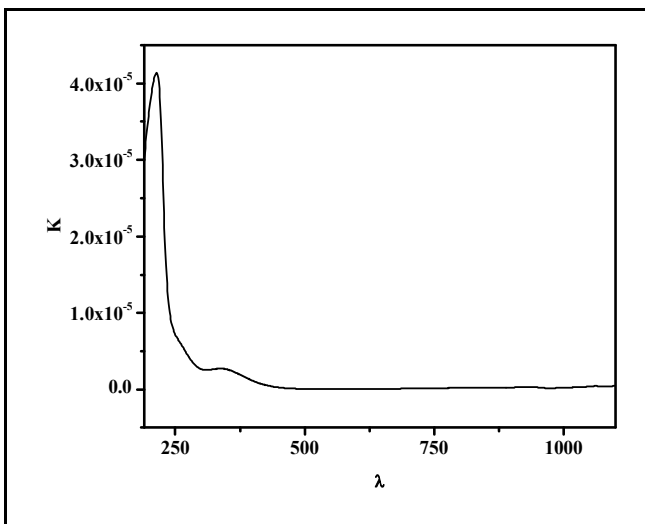
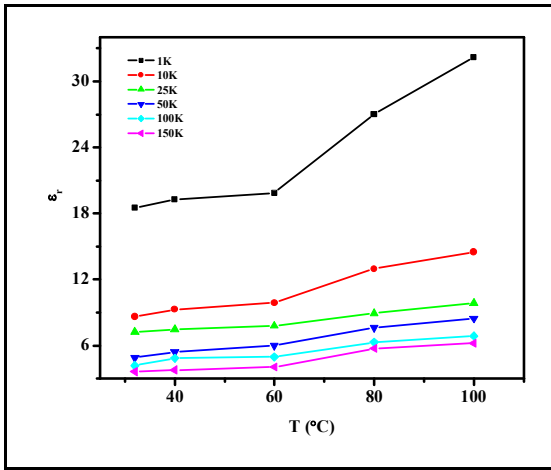


Fig.7: Variation of Wavelength with Extinction coefficient of the grown  $\text{Na}_2\text{SbF}_5$  crystal

## 6. Dielectric Studies

The dielectric constant and dielectric loss of  $\text{Na}_2\text{SbF}_5$  crystal were measured using Agilent 4284A LCR meter.



**Fig. 8: Dielectric constant vs temperature at different frequencies for the grown Na<sub>2</sub>SbF<sub>5</sub> crystal**

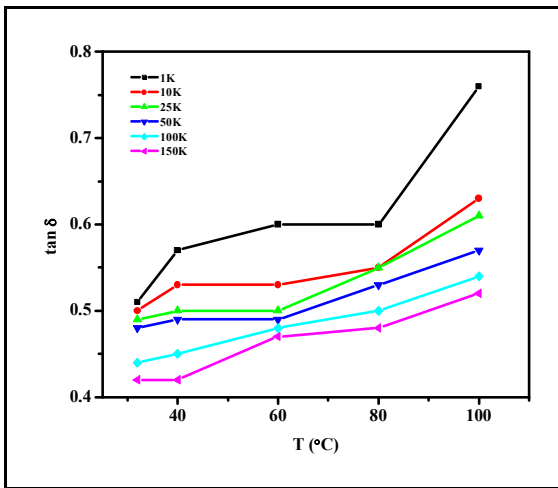


**Fig.9 Dielectric loss vs temperature at different frequencies for the grown Na<sub>2</sub>SbF<sub>5</sub> crystal**

It is observed from the plot (Fig.8) that the dielectric constant decreases exponentially with increasing frequency and then attains almost a constant value in the high frequency region (above 10 KHz). It is also observed that as the temperature increases, the value of the dielectric constant also increases. The same trend is observed in the case of dielectric loss versus frequency (Fig.9). The very high value of dielectric constant at low frequencies may be due to the presence of all the four polarizations namely, space charge, orientation, electronic and ionic polarization and its low value at higher frequencies may be due to the loss of significance of these polarizations gradually [49-51]. From the plot, it is also observed that dielectric constant increases with increasing temperature, attributed to space charge polarization near the grain boundary interfaces, which depends on the purity and perfection of the sample (Balarew et al 1984) [52]. The characteristic of low dielectric loss for a given sample suggests that the sample possesses enhanced optical quality with lesser defects and this parameter is highly important for making this material suitable for various nonlinear optical applications [53-54]. A.C. conductivity varied exponentially with temperature according to the typical activation law,

$$\sigma_{ac} = \sigma_0 e \times p (-E_a/KT) \tag{5}$$

Where  $\sigma_0$  is the pre exponential factor depending on the material,  $E_a$  is the activation energy for ions migration,  $K$  is the Boltzman constant and  $T$  is the absolute temperature. A.C. conductivity was observed to increase with increase in temperature. As temperature rises, due to the creation of more and more defects conductivity increases. Conductivity has smaller values at low frequencies is related to the accumulation of ions due to the slow periodic reversal of the electric field. The variation of AC conductivity with frequencies of applied field has been shown in the Fig. 10.

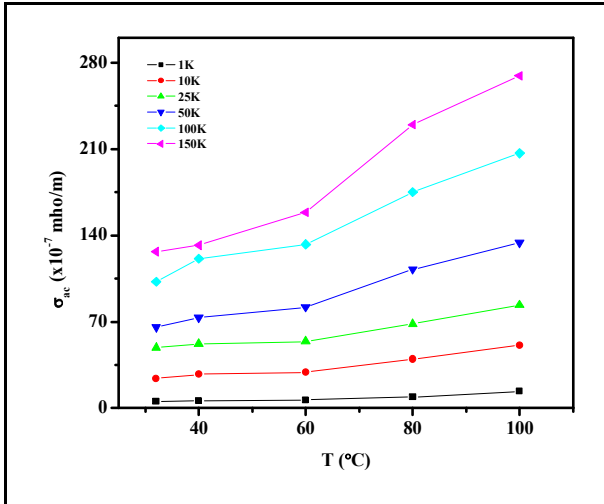


Fig. 10 AC conductivity vs temperature at different frequencies for the grown Na<sub>2</sub>SbF<sub>5</sub> crystal

Arrhenius plot for the grown Na<sub>2</sub>SbF<sub>5</sub> crystal for 1 KHz and 100 KHz has been presented in the Fig. 11 and 12. The activation energy for the grown Na<sub>2</sub>SbF<sub>5</sub> crystal for frequencies 1 KHz and 100 KHz has been found as 0.0032 eV and 0.0026 eV.

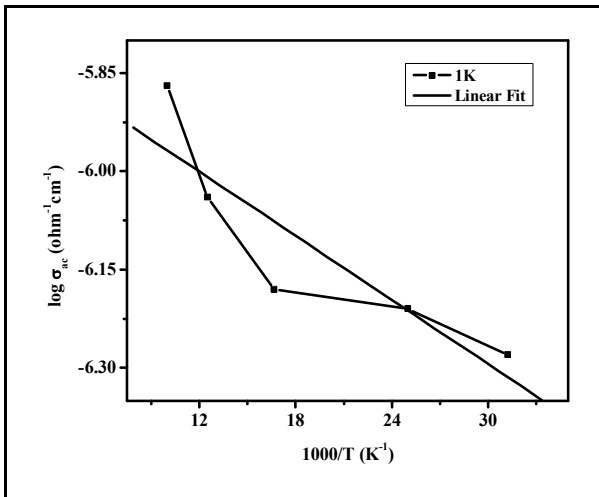


Fig.11 Arrhenius plot for the grown Na<sub>2</sub>SbF<sub>5</sub> crystal at 1 KHz

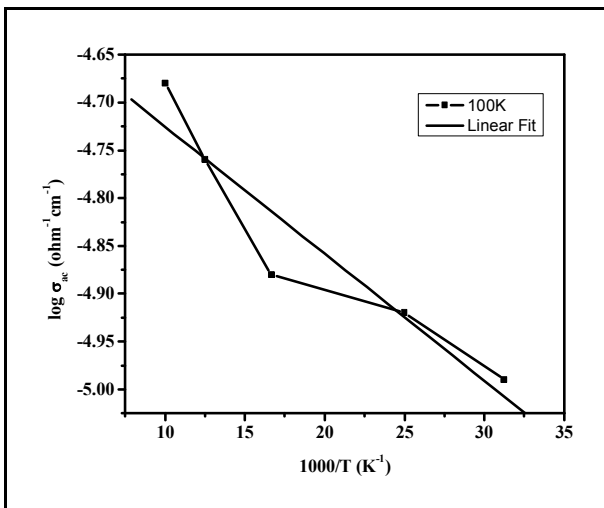


Fig.12 Arrhenius plot for the grown Na<sub>2</sub>SbF<sub>5</sub> crystal at 100 KHz

Theoretical calculations shows that the high frequency dielectric constant is explicitly dependent on the valence electron Plasmon energy, an average energy gap referred to as the Penn gap and the Fermi energy. The Penn gap is determined by fitting the dielectric constant with the Plasmon energy [55].

The molecular weight of the grown crystal is  $M = 263$  g/mol, the total number of valence electron  $Z = 42$ , Density of the grown crystal was found to be  $\rho = 3.59$  g-cm<sup>3</sup> and dielectric constant at  $\epsilon_\infty = 32.18$ . The valence electron plasma energy,  $\hbar\omega_p$  is given by [56-58],

$$\hbar\omega_p = 28.8 \left( \frac{Z\rho}{M} \right)^{\frac{1}{2}} \quad (6)$$

Fermi energy in terms of Plasma energy is given as,

$$E_p = \frac{\hbar\omega_p}{(\epsilon_m - 1)^{\frac{1}{2}}} \quad (7)$$

$$E_F = 0.2948(\hbar\omega_p)^{\frac{4}{3}} \quad (8)$$

Polarizability,  $\alpha$  is obtained using the relation,

$$\alpha = \left[ \frac{(\hbar\omega_p)^2 S_0}{(\hbar\omega_p)^2 S_0 + 3E_p^2} \right] \times \frac{M}{\rho} \times 0.396 \times 10^{-24} \text{ cm}^3 \quad (9)$$

where  $S_0$  is a constant for a particular material, and is given by

$$S_0 = 1 - \left[ \frac{E_p}{4E_F} \right] + \frac{1}{3} \left[ \frac{E_p}{4E_F} \right]^2 \quad (10)$$

The value of  $\alpha$  so obtained agrees well with that of Clausius-Mossotti equation [59], which is given by,

$$\alpha = \frac{3M}{4\pi N_A \rho} \frac{\epsilon_\infty - 1}{\epsilon_\infty + 2} \quad (11)$$

where the symbols have their usual significance.  $N_A$  is Avagadro number and the calculated fundamental data on the grown crystal of  $\text{Na}_2\text{SbF}_5$  are listed in Table.1.

**Table.1 Dielectric parameters of the grown  $\text{Na}_2\text{SbF}_5$  crystal**

Parameters	Values
Plasma energy (eV)	6.77
Penn gap (eV)	1.21
Fermi gap (eV)	3.75
Polarizability (cm <sup>-3</sup> ) using Penn analysis	6.61 x 10 <sup>-24</sup>
Polarizability (cm <sup>-3</sup> ) using Clausius Mossotti Equation	2.65 x 10 <sup>-23</sup>

## 7. Nlo Studies

The Kurtz and Perry technique is the most widely used technique which is used to confirm the SHG efficiency of NLO materials [59]. For this study, a finely grounded crystal in powder form was taken in a capillary tube. The fundamental beam of 1064 nm from Q- switched Nd:YAG laser beam and 10 ns pulse width with an input rate of 10 Hz was used to test the NLO property of the sample. The second harmonic signal generated in the crystalline sample was confirmed by the emission of green radiation from the crystal. The crystals of  $\text{Na}_2\text{SbF}_5$  were grinded to uniform particle size of about 125 – 150  $\mu\text{m}$  were taken and packed in capillaries of uniform bore and then exposed to the laser radiation. The powder of potassium dihydrogen phosphate (KDP) with the same particle size was used as the reference. The output of the grown crystal measured as the 2.34 mJ while the KDP gave an SHG signal of 8.8 mJ for the same input beam of energy of 0.68 J. The NLO efficiency of  $\text{Na}_2\text{SbF}_5$  crystal is observed to be 0.265 times that of the standard KDP crystal.

## 8. Conclusion

Sodium Penta Fluoro Antimonate ( $\text{Na}_2\text{SbF}_5$ ) crystal has been grown by slow evaporation technique using deionized water as solvent. The crystallinity nature of the given crystal has been confirmed with the help

of XRD analysis. It crystallized in orthorhombic system with lattice parameters  $a = 5.453 \text{ \AA}$ ,  $b = 8.006 \text{ \AA}$ ,  $c = 11.133 \text{ \AA}$ ,  $\alpha = \beta = \gamma = 90^\circ$  and has the space group of  $P2_12_12_1$ . The functional group of the sample has been determined by FTIR analysis. High degree of transparency is observed in the visible region as well as UV region and has a lower cut-off wavelength of 311 nm. The band gap energy is found to be 5.3 eV using Tauc's plot. Using dielectric studies the plasma energy, Penn gap, Fermi gap and polarizability has been tabulated. The NLO efficiency of  $\text{Na}_2\text{SbF}_5$  crystal is observed to be 0.265 times that of the KDP crystal.

## References

1. J. Benet Charles, F.D. Gnanam and K. Sivakumar, *Mat. Chem. & Phys.*, 38 (1994) 337- 341
2. Zoran Mazej and Rika Hagiwara, *J. Flu. Chem.*, 128 (2007) 423-437
3. Alenka Turicnik, Primoz Benkic and Boris Zemva, *J. Flu. Chem.*, 121 (2003) 245-251
4. M. Ponvikar, B. Sedej, B. Pihlar and B. Zemva, *Anal. Chim. Acta*, 418 (2000) 113-118
5. J. Burgess, R.D. Peacock and R. Sherry, *J. Flu. Chem.*, 20 (1982) 541-554
6. M.P. Borzenkova, F.V. Kalinchenko and A.V. Novoselova, *Zh. Neorg. Khim.*, 29 (1984) 703-705
7. Yu.N. Moskvich, B.I. Cherkasov, A.M. Polykav, A.A. Sukhovskii and R.L. Davidovich, *Phy. Stat. Sol.*, (b) 156 (1989) 615-631
8. V.Ya. Kavun, L.A. Zemnukhova, V.I. Soriano, T.A. Kaidalova, R.L. Davidovich and N.I. Sorokin, *Russ. Chem. Bull.*, 51 (2002) 1996-2002.
9. R. Mary Jenila, T.R. Rajasekaran and J. Benet Charles, *Sci. Acta Xav.*, 3 (2012) 1-10
10. Elsammo Chacko, J. Mary Linet and S. Mary Navis Priya, *Ind. J. Pure & App. Phys.*, 44 (2006) 260-263
11. J.G. Bergman, G.R. Crane and H. Guggenheim, *J. App. Phys.*, 46 (1975) 4645
12. R. Mary Jenila, T.R. Rajasekaran and J. Benet Charles, *Sch. Res. Lib., Arch. App. Sci. Res.*, 4(4) (2012) 1850-1856
13. Rani Christhu Dhas, J. Benet Charles and F.D. Gnanam, *J. Crys. Growth.*, 137 (1994) 295-298
14. V. Ya. Kavun, V.I. Sergienko, N.I. Sorokin, L.A. Zemnukhova, T.A. Kaidalova and E.B. Merkulov, *J. Str. Chem.*, 42 (2001) 570
15. N.V. Makarenko, A.A. Udovenko, L.A.Zemnukhova, V.Ya. Kavun and M.M. Polyantsev, *J. Flu. Chem.*, 168 (2014) 184-188
16. Karl O. Christe, William W. Wilson, Roland A. Bougon and Pierrette Charpin, *J. Flu. Chem.*, 34 (1987) 287-298
17. W.H.J. de Beer and A.M. Heyns, *Sol. Stat. Comm.*, 33 (1980) 31-34
18. D. Tichit, B. Ducourant, R. Fourcade and G. Mascherpa, *J. Flu. Chem.*, 13 (1979) 45-53
19. N. Habibi, B. Ducourant, B. Bonnet and R. Fourcade, *J. Flu. Chem.*, 12 (1978) 63-72
20. T. Bircharl and B. Dellavalle, *Can. J. Chem.*, 49 (1971) 2808
21. K. Yamada, Y. Ohnuki, H. Ohki and T. Okuda, *Chem. Lett.*, 5 (1999) 627
22. Bystroem and K.A. Wilhelmi, *Ark. Kemi*, 3 (1951) 17
23. G.V. Zimina, L.A. Sadokhina and V.E. Plyushchev, *Rus. J. Inorg. Chem.*, 21 (1976) 748-750
24. N. Habibi, B. Bonnet and B. Ducourant, *J. Flu. Chem.*, 12 (1987) 237-247
25. J. Benet Charles and F.D. Gnanam, *Mat. Chem. & Phys.*, 38 (1994) 337
26. R. Fourcade, G. Mascherpa and E. Philippot, *Acta Crys. (b)*, 31 (1975) 2322-2327
27. R. Fourcade, G. Mascherpa and B. Ducourant, *Rev. Chim. Min.*, 20 (1983) 837-844
28. A. Cyrac Peter, M. Vimalan, P. Sagayaraj and J. Madhavan, *Sch. Res. Lib., Arch. App. Sci. Res.*, 2(1) (2010) 191-197
29. C. Besky Job, R. Shabu and S. Paulraj, *Int. J. Eng. & App. Sci.*, 2 (2015) 26-29
30. Seichii Miyajima, Nobuo Nakamura and Hideaki Chihara, *J. Phy. Soc. Jap.*, 49 (1980) 1867-1873
31. L.A. Zemnukhova, R.L. Davidovich, P.S. Gordienko, J. Grigas, A.N. Kovrianov, S.I. Kuznetsov, T.A. Kaidalova and V. Urbonavicius, *Phys. Stat. Sol. (a)*, 80 (1983) 553-558
32. L.M. Avkhutski, R.L. Davidovich, L.A.Zemnukhova, P.S. Gordienko, V. Urbonavicius and J. Grigas, *Phys. Stat. Sol.*, (b) 116 (1983) 483-488
33. P. Abjean, M. Leblanc, R. Depape and G. Fercy, *Acta Crys.*, C41 (1985) 1696-1698
34. P. Gravereau, C. Mirambet, L. Fournier, J. Granec and L.Lozano, *Acta Crys.*, C46 (1990) 2294-2297
35. R. Fourcade, G. Mascherpa, E. Philippot and M. Maurin, *Rev. Chim. Min.*, 11 (1974) 481-482
36. F.B. Kalinchenko, M.P. Borzenkova and A.V. Novoselova, *Russ. J. Inorg. Chem.*, 27 (1982) 1653

37. N.M. Laptash, E.V. Kovaleva, A.A. Mashkovskii, A.Yu. Belolipstev and L.A. Zemnukhova, *J. Str. Chem.*, 48 (2007) 848-854
38. J. Benet Charles, *Mat. Chem. & Phys.*, 45 (1996) 189-192
39. J.G. Bergman and G.R. Crane, *J. Chem. Phys.*, 60 (1974) 2470
40. J.G. Bergman, G.R. Crane and E.H. Turner, *J. Sol. Stat. Chem.*, 21 (1977) 127
41. J.G. Bergman, D.S. Chemla, R. Fourcade and G. Mascherpa, *J. Sol. Stat. Chem.*, 23 (1978) 187-190
42. S. Gunasekaran, G. Anand, R. Arun Balaji, J. Dhanalakshmi, S. Kumaresan and G. Anbalagan, *Int. J. Chem. Tech. Res.*, 1 (2009) 649-653
43. T.G. Belicheva and N.I. Roi, *Russ. J. Inorg. Chem.*, 17 (1972) 74-77
44. L. Botto and A.C. Garcia, *Mat. Res. Bull.*, 24 (1989) 1431-1439
45. Kazuo Nakamoto, *Infrared and Raman spectra of Inorganic and Coordination Compounds*, John Wiley & Sons, Newyork, 1986.
46. L.A. Zemnukhova, R.L. Davidovich, A.A. Udovenko and E.V. Kovaleva, *Russ. J. Coord. Chem.*, 31 (2005) 115-120
47. V. Kannan, R. Bairava Ganesh, P. Ramasamy, *Cryst. Growth Des.* 6 (2006) 1876-1880.
48. F. Moser and F. Urbach, *Phys. Rev.*, 102 (1956) 1519-1523
49. P.C. Thomas, S. Aruna, J. Packiam Julius, A. Joseph Arul Pragasam, P. Sagayaraj, *Crys. Res. Tech.*, 41 (2006)1231- 1235
50. B. Narsimha, R.N. Choudhary and K.V. Rao, *Mater. Sci.* 23 (1988) 1416
51. K.V. Rao and A. Smakula, *J. App. Phys.*, 36 (1965) 2031- 2038.
52. C. Balarew, R. Duhlew, *J. Sol. Stat. Chem.*, 55 (1984)
53. Suresh Sagadevan, *Int. J. Curr. Eng. & Tech.*, 4 (2014) 2447-2449
54. U. Von Hundelshausen, *Phys. Lett.*, 34 (A) (1971) 405-406.
55. N.M. Ravindra, R.P. Bharadwaj, K. Sunil Kumar and V.K. Srivastava, *Infrared Phys.*, 21 (1981) 369.
56. S. Suresh and D. Arivuoli, *J. Opt. Elec. & Bio. Med. Mat.*, 3 (2011) 63-68
57. N.M. Ravindra and V.K. Srivastava, *Infrared Phys.*, 20 (1980) 67
58. D.R. Penn, *Phys. Rev.*, 128 (1962) 2093
59. S.K. Kurtz and T.T. Perry, *A Powder Technique For The Evaluation of Nonlinear Optical Materials*, *J. App. Phys.*, 39 (1968) 3798-3813

\*\*\*\*\*